

## Hierarchical strontium carbonate submicron spheres self-assembled under hydrothermal conditions

Wancheng Zhu\*<sup>1</sup>, Guanglei Zhang<sup>1</sup>, Chunming Liu<sup>1</sup>, Qiang Zhang\*\*<sup>2</sup>, and Shenlin Zhu<sup>2</sup>

<sup>1</sup> Department of Chemical Engineering, Qufu Normal University, Shandong 273165, P. R. China

<sup>2</sup> Department of Chemical Engineering, Tsinghua University, Beijing 100084, P. R. China

Received 12 December 2009, revised 2 June 2010, accepted 6 June 2010

Published online 18 June 2010

**Key words** strontium carbonate, hierarchical, spheres, self-assembly, hydrothermal.

Uniform hierarchical strontium carbonate ( $\text{SrCO}_3$ ) submicron spheres bearing detectable cavities on the surfaces and porous structures within the body were efficiently obtained, by a facile hydrothermal treatment (190 °C, 12 h) of the room temperature precipitate derived from  $\text{Na}_2\text{CO}_3$  and  $\text{SrCl}_2$  solution.  $\text{MgCl}_2$  and ethylene diamine tetraacetic acid (EDTA) disodium salt were used as the additives. The as-obtained submicron spheres were self-assembled by crystalline  $\text{SrCO}_3$  nanoparticles under hydrothermal conditions. The present hydrothermally synthesized hierarchical  $\text{SrCO}_3$  submicron spheres would enlarge the potentials of  $\text{SrCO}_3$  micro-/nanostructures in the hierarchical architectures and porous materials family for further applications in the fields of catalysis, composites, adsorbents, and devices, etc.

© 2010 WILEY-VCH Verlag GmbH & Co. KGaA, Weinheim

### 1 Introduction

Complex architectures, especially three-dimensional hierarchical architectures have attracted extraordinary attention and intensive interests due to their unique structures and fantastic properties different from those of the monomorph structures [1]. The hierarchical structures are expected to play a significant role in fabricating the high performance nanocomposites [2], energy conversion and storage device [3], efficient catalyst [4], and adsorbent for water treatment [5].

Recently, three-dimensional hierarchical architectures of strontium carbonate ( $\text{SrCO}_3$ ), such as flowerlike [6,7], bundle-like, dumbbell-like, hexagonal star-like [8,9], branch-like [10], especially spherical or sphere-like [7-9,11,12]  $\text{SrCO}_3$  microstructures, have attracted extraordinary attention due to their novel applications as chemiluminescence sensors [13], catalyst [14,15], etc., in addition to their traditional utilizations as additives in the production of iridescent and specialty glasses for color television tubes, strontium metal and other strontium compounds [16,17].  $\text{SrCO}_3$  microspheres bearing smooth surfaces could be formed by enzyme-catalyzed decomposition [11], room temperature aging method in presence of appropriate additives, such as poly-(styrene-alt-maleic acid) (PSMA) [8] and ethylene diamine tetraacetic acid (EDTA) [9], and also microemulsion-mediated solvothermal synthesis in presence of cetyltrimethylammonium bromide (CTAB) [12]. Very recently, mesoporous  $\text{SrCO}_3$  spheres derived from room temperature ionic liquid (ILs) [18] and hierarchical  $\text{SrCO}_3$  architectures originated from room temperature aging method (5 days) based on the conversion of pre-synthesized  $\text{SrCrO}_4$  nanowires [19] have also been reported. In contrast, facile synthesis of  $\text{SrCO}_3$  submicron spheres in aqueous solution within a short time is still an open question.

On the other hand, as one of the most efficient methods of soft chemistry, hydrothermal technologies have been widely employed in the process of one-dimensional (1D) nanostructures [20-22] because of the distinct advantages over other traditional methods [23]. Most recently, hydrothermal method has also been emerged as a thriving technique for the facile fabrication of the complex hierarchical architectures, such as cantaloupe-like  $\text{AlOOH}$  superstructures [24], hierarchical  $\text{Ni}(\text{OH})_2/\text{NiO}$  hollow architectures [25], hierarchical  $\text{Bi}_2\text{WO}_6$  microspheres [26] and octahedron-like structures [27], monodispersed colloidal carbon spheres [28], and hierarchical  $\text{InVO}_4$  mesoporous microspheres [29]. In this contribution, we report a facile hydrothermal

\* Corresponding author: e-mail: zhuwancheng@tsinghua.org.cn

\*\* Present address: Fritz-Haber-Institut der Max-Planck-Gesellschaft, Faradayweg 4–6, 14195 Berlin, Germany

strategy for hierarchical SrCO<sub>3</sub> submicron spheres with detectable cavities on the surfaces and porous structures within the body, which are self-assembled by related nanoparticles under hydrothermal conditions in presence of EDTA disodium salt and MgCl<sub>2</sub> as additives.

## 2 Experimental

**Synthesis** SrCO<sub>3</sub> submicron spheres were synthesized via a room temperature coprecipitation of SrCl<sub>2</sub> and Na<sub>2</sub>CO<sub>3</sub> followed by a facile hydrothermal treatment, in presence of appropriate amount of MgCl<sub>2</sub> and EDTA disodium salt as additives. In a typical procedure, Na<sub>2</sub>CO<sub>3</sub> (1.41 mol·L<sup>-1</sup>, 10 mL) was dropped into SrCl<sub>2</sub> (1.41 mol·L<sup>-1</sup>, 11 mL) under vigorous magnetic stirring at room temperature (dropping rate: 1 droplet per sec approx), leading to a white slurry. EDTA disodium salt (0.4187 g) and MgCl<sub>2</sub>·6H<sub>2</sub>O (0.1398 g) were added into the previously resultant and continuously stirred slurry, keeping molar ratios of EDTA disodium salt as well as MgCl<sub>2</sub> to Na<sub>2</sub>CO<sub>3</sub> as 5%. The slurry was supplied deionized (DI) water to 55 mL and kept stirring for another 3 min., and then transferred into a Teflon-lined stainless steel autoclave with a capacity of 70 mL. The autoclave was sealed and heated (1 K min<sup>-1</sup>) to 190 °C and kept in an isothermal state for 12 h and then cooled down to room temperature naturally. The precipitate was filtered, washed with DI water and absolute alcohol for three times, respectively, and finally dried (120 °C, 6 h) for further characterization.

**Characterization** Crystal phase and structure of the sample were identified by the X-ray powder diffractometer (XRD, D/MAX 2500, Rigaku, Japan) using a Cu K<sub>α</sub> radiation. Morphology, microstructure and composition of the samples were examined by the field emission scanning electron microscopy (SEM, JSM 7401F, JEOL, Japan) operated at 3.0 kV, and a high resolution transmission electron microscopy (TEM, JEM-2010, JEOL, Japan) performed at 120.0 kV equipped with an X-ray energy dispersive spectrometer (EDS, INCA Energy TEM, Oxford Instruments, UK) and a charge coupled device (CCD) camera (Orius SC 1000, Gatan, USA). For TEM and EDS analyses, the sample was first dispersed in ethanol by ultrasonic treatment for 15 min and then deposited onto the holey carbon film supported by a copper grid. The thermal decomposition behavior of the sample was detected by the thermo-gravimetric analyzer (TGA, Netzsch STA 409C, Germany) carried out in dynamic air with a heating rate of 10.0 K min<sup>-1</sup>. Size distribution of the submicron spheres was estimated by direct measuring about 200 particles from the typical SEM images. Ultraviolet-visible (UV-vis) absorption spectra were recorded by a Varian Cary-300 spectrophotometer.

## 3 Results and discussion

XRD patterns, SEM images and size distribution of the hydrothermal product (190 °C, 12 h) in absence or presence of additives are shown in figure 1. Hydrothermal treatment of the slurry containing the room temperature coprecipitation in absence of additives led to polyhedron-like orthorhombic SrCO<sub>3</sub> (Fig. 1a<sub>1</sub>) particles with well-defined facets and distinct wide size distribution (Fig. 1b). In contrast, hydrothermal treatment of the same slurry in presence of additives (EDTA disodium salt and MgCl<sub>2</sub>) resulted in orthorhombic SrCO<sub>3</sub> (Fig. 1a<sub>2</sub>) submicron spheres with a uniform hierarchical structure bearing detectable cavities on the surfaces (Fig. 1c,c<sub>1</sub>) and also a narrow size distribution (Fig. 1d). It can be seen that, whether the additives are present or not, all diffraction peaks of the XRD patterns (Fig. 1a<sub>1-2</sub>) could be readily indexed to the orthorhombic phase of SrCO<sub>3</sub> (strontianite, PDF# 05-0418). The distinct difference between the diffraction intensity of the XRD patterns might be attributed to the differences of the morphology especially the average size of the hydrothermal product. The remarkable broadening of the diffraction peaks of the XRD pattern (Fig. 1a<sub>2</sub>) revealed the existence of crystalline SrCO<sub>3</sub> nanoparticles within the submicron spherical structure, in accordance with the SEM observation (Fig. 1c,c<sub>1</sub>). Meanwhile, the crystallite size along the [111] direction ( $D_{111}$ ) calculated by the Debye-Scherrer equation was 14.5 nm. Thus, the hydrothermal treatment of the room temperature precipitate in presence of appropriate EDTA disodium salt and MgCl<sub>2</sub> as additives didn't alter the chemical composition whereas greatly influenced the morphology of the hydrothermal product. The specific morphology of the present hierarchical SrCO<sub>3</sub> submicron spheres was somewhat like the spherical SrCO<sub>3</sub> with smooth surface reported in the literature by other methods [8,9,11,12], and quite similar to the mesoporous SrCO<sub>3</sub> spheres obtained in room temperature ILs [18]. Meanwhile, the statistical data (Fig.1d) demonstrated that, approx 95% of the hierarchical SrCO<sub>3</sub> submicron spheres had a diameter within the range of 600 nm to 1100 nm, indicating a narrower diameter distribution compared with that of the mesoporous SrCO<sub>3</sub> spheres

obtained in ILs containing two types of spheres with a diameter of 300–400 nm and 60–100 nm [18].

Formation of the hierarchical  $\text{SrCO}_3$  submicron spheres could be expressed in ionic form as follows:

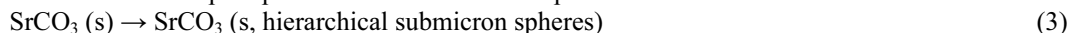
Room temperature coprecipitation of  $\text{Na}_2\text{CO}_3$  and  $\text{SrCl}_2$ :



Hydrothermal treatment of the precipitate at 190 °C for 12 h in absence of additives:



Hydrothermal treatment of the precipitate at 190 °C for 12 h in presence of additives:



It was worth noting that,  $\text{Na}^+$  (a.q.) as well as  $\text{Cl}^-$  (a.q.) was remained in the reactant system during the room temperature coprecipitation and subsequent hydrothermal treatment, and finally removed by post treatment such as filtration and washing after the hydrothermal treatment. On the other hand, to avoid the introduction of unwanted impurity  $\text{MgCO}_3$  by the possible side reaction between  $\text{Na}_2\text{CO}_3$  and  $\text{MgCl}_2$ ,  $\text{Na}_2\text{CO}_3$  was dropped into  $\text{SrCl}_2$  solution, and the amount of  $\text{SrCl}_2$  was strictly kept relatively excessive corresponding to that of  $\text{Na}_2\text{CO}_3$ , in particular, the additives were added into the system after the accomplishment of  $\text{Na}_2\text{CO}_3$  feeding. Thus,  $\text{Mg}^{2+}$  was also remained within the reaction system during the hydrothermal treatment and ultimately removed by subsequent filtration and washing.

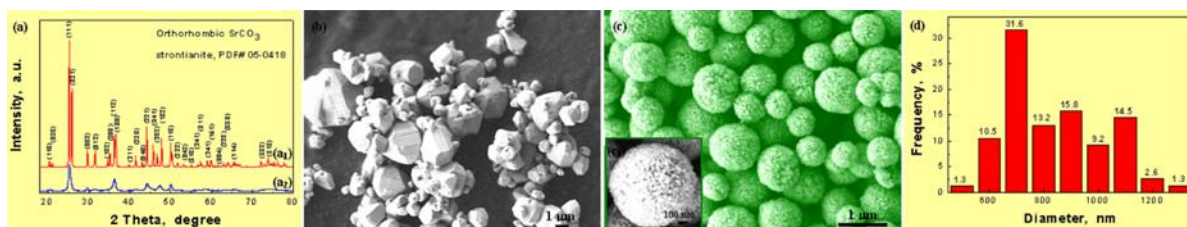


**Fig. 1** XRD patterns (a), SEM images (b–c) and size distribution (d) of the hydrothermal product obtained in absence (a<sub>1</sub>, b) or presence (a<sub>2</sub>, c, c<sub>1</sub>, d) of EDTA disodium salt and  $\text{MgCl}_2$  as additives (molar ratio, additives: $\text{Na}_2\text{CO}_3$  =5:100,  $\text{SrCl}_2$ : $\text{Na}_2\text{CO}_3$  =1.1:1, 190 °C, 12.0 h). Inserted figure (c<sub>1</sub>) shows a high resolution SEM image of the  $\text{SrCO}_3$  submicron spheres. (Online color at [www.crt-journal.org](http://www.crt-journal.org))

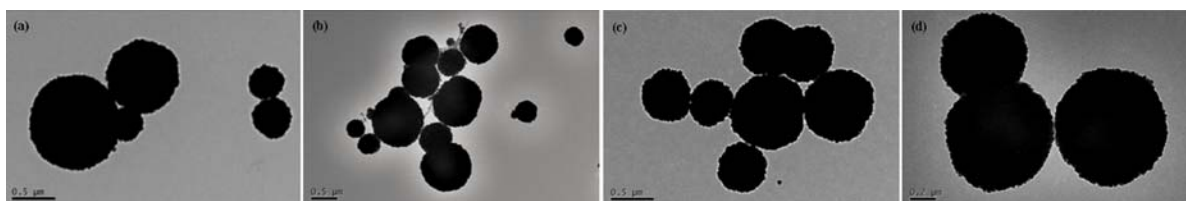
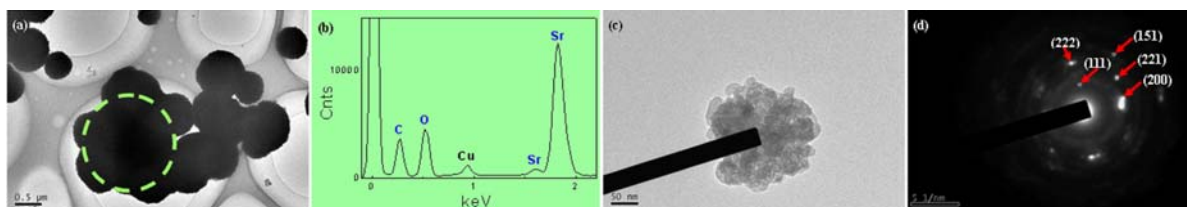


**Fig. 2** Effects of the molar ratio of  $\text{SrCl}_2$ : $\text{Na}_2\text{CO}_3$  on the morphology and size distribution of the hydrothermally synthesized submicron  $\text{SrCO}_3$  spheres. Temperature (°C): 190; Time (h): 12.0; EDTA disodium salt: $\text{Na}_2\text{CO}_3$  =5:100;  $\text{MgCl}_2$ : $\text{Na}_2\text{CO}_3$  =5:100;  $\text{SrCl}_2$ : $\text{Na}_2\text{CO}_3$  =1.02:1 (a), 1.05:1 (b), 1.2:1 (c), 1.1:1 (d).

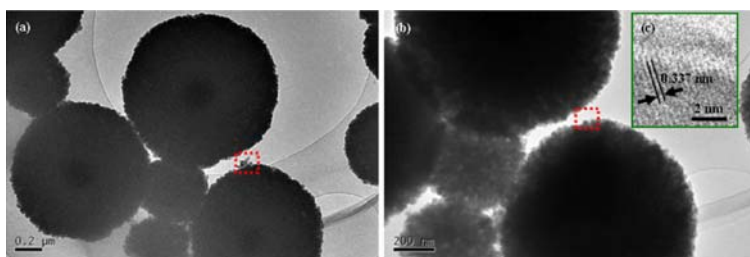
Molar ratio of the reactants, i.e.  $\text{SrCl}_2$ : $\text{Na}_2\text{CO}_3$ , has significant effect on the morphology and size distribution of the hydrothermally synthesized  $\text{SrCO}_3$  submicron spheres (190 °C, 12.0 h), as shown in figure 2. When the molar ratio of the reactants  $\text{SrCl}_2$ : $\text{Na}_2\text{CO}_3$  changed within the range of 1.02:1–1.2:1 (Fig. 2a–d), 1.1:1 (Fig. 2d) was proved as the optimum molar ratio needed for the hydrothermal formation of the uniform hierarchical submicron spheres with narrow size distribution, with the molar ratio of the additive EDTA disodium salt, as well as  $\text{MgCl}_2$  to  $\text{Na}_2\text{CO}_3$  kept as 5:100. Meanwhile, the pH value of the solution phase was slightly dropped down from original ca. 6.2 to final ca. 5.8–5.9 during the hydrothermal treatment, revealing the weak acidic environment necessary for the formation of the uniform hierarchical  $\text{SrCO}_3$  submicron spheres.

Figure 3 shows the TEM images, corresponding EDS spectrum and selected area electron diffraction (SAED) pattern of the hierarchical submicron  $\text{SrCO}_3$  spheres. TEM images (Fig. 3a,c) indicated the hierarchical architectures of uniform spherical morphology. EDS spectrum (Fig. 3b) recorded from the focused section (denoted as the dashed green circle) of the spheres hanging within the hole of the holey carbon film (Fig. 3a) definitely indicated that the submicron spheres comprised Sr, C and O, taking into consideration the background element Cu derived from the employed copper grid. A small submicron sphere (diameter: ca. 200 nm) was particularly selected for a closer observation with a higher magnification, so as to be feasible for

the SAED performance. The high magnification TEM image (Fig. 3c) clearly showed that the selected small submicron sphere was aggregated by multitudinal nanoparticles (diameter: 20–40 nm), and the assembly even left some detective pores with a diameter of ca. 10 nm not only on or near the surface but also within the inner of the sphere. Meanwhile, the corresponding SAED pattern (Fig. 3d) exerted some regularly aligned bright spots and also blur diffraction rings, indicating the crystalline phase of the nanoparticles within the submicron spheres, and the blur diffraction rings containing relatively bright spots could be indexed as the planes of (111), (200), (221), (222) and (151), which were thus in agreement with the previous XRD results (Fig. 1a<sub>2</sub>). Although the submicron spheres looked like the agglomeration of SrCO<sub>3</sub> nanoparticles (in other words, loosely attached nanoparticles), the uniform hierarchical SrCO<sub>3</sub> submicron spheres were believed to be self-assembled by the related crystalline nanoparticles in presence of appropriate additives, rather than the random agglomeration.



**Fig. 3** TEM images (a, c), EDS spectrum (b) and SAED pattern (d) of the hydrothermally synthesized SrCO<sub>3</sub> submicron spheres deposited onto the holey carbon film (a, b) or ordinary carbon film (c, d) supported by a copper grid (molar ratio, additives: Na<sub>2</sub>CO<sub>3</sub>=5:100, SrCl<sub>2</sub>:Na<sub>2</sub>CO<sub>3</sub>=1.1:1, 190 °C, 12.0 h). (Online color at [www.crt-journal.org](http://www.crt-journal.org))



**Fig. 4** Higher magnification TEM images (a, b) and HRTEM image (c) of the hydrothermally synthesized SrCO<sub>3</sub> submicron spheres deposited onto the holey carbon film, supported by a copper grid (molar ratio, additives: Na<sub>2</sub>CO<sub>3</sub>=5:100, SrCl<sub>2</sub>:Na<sub>2</sub>CO<sub>3</sub>=1.1:1, 190 °C, 12.0 h).

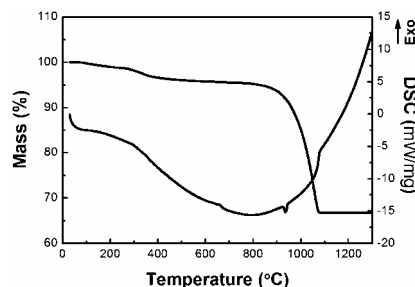


**Fig. 5** TG-DSC curves of the hydrothermally synthesized SrCO<sub>3</sub> submicron spheres (molar ratio, additives: Na<sub>2</sub>CO<sub>3</sub>=5:100, SrCl<sub>2</sub>:Na<sub>2</sub>CO<sub>3</sub>=1.1:1, 190 °C, 12.0 h).

Evolution behavior of the nanoparticles attached to the SrCO<sub>3</sub> submicron spheres under the irradiation of the electron beam was recorded, as shown by the red dotted-line rectangular region in figure 4. Several nanoparticles assembled into a cross-hands profile were selected and then focused with the electron beam (Fig. 4a). With the irradiation time went on, the focused nanoparticles gradually bent over, further inclined to the surface, and finally embedded into the submicron sphere (Fig. 4b), definitely indicating the porous structure existed within the submicron spheres. As a matter of fact, SEM (Fig. 1c,c<sub>1</sub>) and TEM (Fig. 3c, Fig. 4a) images also confirmed the porous structures within the submicron spheres, which prefigured the potential applications of the present SrCO<sub>3</sub> submicron spheres as the support of the catalyst and also the adsorbents for the pigment-containing effluent treatment. Meanwhile, within the red dotted-line rectangular region of the submicron sphere surface (Fig. 4b), there interplanar spacings of 0.337 nm detected from the legible lattice fringes (Fig. 4c), quite similar to that of the (021) planes for the stand orthorhombic SrCO<sub>3</sub>. After irradiated by the electron beam for some long time, the submicron sphere got a relatively smooth surface. This is helpful for understanding the hydrothermal effect on the formation of the hierarchical SrCO<sub>3</sub> submicron spheres, which created an environment of high temperature and high pressure and thus facile for the transportation of the building blocks.

Figure 5 shows the TG-DSC curves of the hydrothermally synthesized SrCO<sub>3</sub> submicron spheres. The mass of the samples decreased from 99.95% (30 °C) to 98.19% (300 °C) to 96.58% (400 °C), then to 93.67 (900 °C),

finally to 66.77% (1100 °C) and kept constant thereafter. The mass loss of 3.38% before the temperature as 400 °C might be attributed to the loss of the adsorbed water, and the subsequent mass loss of 29.81% between the temperature range of 400-1100 °C was owing to the thermal decomposition of SrCO<sub>3</sub>:



The corresponding mass loss was quite similar to the theoretical value of the mass loss of the above decomposition (29.81%), and almost the same with that occurred for the thermal decomposition of the high pure SrCO<sub>3</sub> phase between 900-1150 °C [30]. The relatively low decomposition temperature of the present SrCO<sub>3</sub> submicron spheres might be ascribed to the size effect of the nanoparticles existed within the submicron spheres. Meanwhile, the DSC curve indicates that there existed a broad endothermic vale within the whole temperature range of the heating procedure especially between 400-1100 °C, which also contains a remarkable endothermic peak at the temperature of 935.3 °C related to the conversion from the orthorhombic  $\alpha$ -SrCO<sub>3</sub> phase to the trigonal  $\beta$ -SrCO<sub>3</sub> phase [30].

The UV-vis absorption spectra (not shown here) recorded from the uniform hierarchical SrCO<sub>3</sub> submicron spheres demonstrated that, the spectra was entirely featureless and there existed no obvious absorption edge in the wavelength range of 200-350 nm, indicating that the uniform hierarchical SrCO<sub>3</sub> submicron spheres were transparent within the ultraviolet region [31].

The nanocrystals existing within the submicron spheres, revealed by the XRD pattern (Fig. 1a<sub>2</sub>), the small spherical aggregates (Fig. 3c) and also the quasi polycrystalline characteristic SAED pattern (Fig. 3d), prefigured the probable assembling behavior of the related nanoparticles in course of the hydrothermal formation of the uniform hierarchical SrCO<sub>3</sub> submicron spheres in presence of additives. In addition, for our case, EDTA disodium salt and MgCl<sub>2</sub> were both required for the hydrothermal formation of the present hierarchical SrCO<sub>3</sub> submicron spheres, and the specific assembly mechanism for the nanoparticles into the uniform hierarchical submicron spheres in presence of the additives was still under investigation. Besides, compared with literature results, the present SrCO<sub>3</sub> submicron spheres containing porous structures are distinctly different with the previously reported smooth-surface SrCO<sub>3</sub> spheres [8,9,11,12] and also those SrCO<sub>3</sub> architectures of other morphologies [6-10], thus suggested new potential applications of SrCO<sub>3</sub> in the fields such as catalysts, composites, adsorbents, and devices. Moreover, the employed hydrothermal synthesis does not need much organic solvents or ILs, thus is an efficient promising and alternative green synthetic route to the hierarchical SrCO<sub>3</sub> architectures, which can also be extended to the preparation of other carbonates with similar structures.

## 4 Conclusion

In summary, uniform hierarchical SrCO<sub>3</sub> submicron spheres bearing detective cavities on the surfaces and porous structures within the body, with a diameter within the range of 600 to 1100 nm and a narrow diameter distribution, were efficiently obtained by a facile hydrothermal treatment (190 °C, 12 h) of the room temperature precipitate derived from Na<sub>2</sub>CO<sub>3</sub> and SrCl<sub>2</sub> solution in presence of appropriate amount of MgCl<sub>2</sub> and EDTA disodium salt as additives. The present uniform hierarchical SrCO<sub>3</sub> submicron spheres were self-assembled by the related crystalline nanoparticles under hydrothermal conditions, assisted by the additives, and the novel hierarchical structures would enlarge the potential applications of SrCO<sub>3</sub> micro/nanostructures in the hierarchical architectures and porous materials family as catalysts, composites, adsorbents, and devices, etc. Moreover, the developed facile hydrothermal strategy may also be expected for the preparation of other carbonates with similar hierarchical porous structures.

**Acknowledgements** This work was supported by the State Key Laboratory of Chemical Engineering (No. SKL-ChE-09A02) and also the Youth Foundation of Qufu Normal University (XJ200926). The authors thank Dr. Meng-Qiang Zhao and associate professor Ling Hu at Beijing Key Laboratory of Green Reaction Engineering and Technology, Department of Chemical Engineering, Tsinghua University, China, for their great help in the TEM characterization, and also appreciate the reviewers for the constructive suggestions on the great improvement of the work.

## References

- [1] X. X. Xu, X. Wang, A. Nisar, X. Liang, J. Zhuang, S. Hu, and Y. Zhuang, *Adv. Mater.* **20**, 3702 (2008).
- [2] M. Q. Zhao, Q. Zhang, X. L. Jia, J. Q. Huang, Y. H. Zhang, and F. Wei, *Adv. Funct. Mater.* **20**, 677 (2010).

- [3] D. S. Su and R. Schlogl, *Chem. Sus. Chem.* **3**, 136 (2010).
- [4] J. Zhu, Y. Cui, Y. Wang, and F. Wei, *Chem. Commun.* **45**, 3282 (2009).
- [5] Y. J. Xu, G. Weinberg, X. Liu, O. Timpe, R. Schlogl, and D. S. Su, *Adv. Funct. Mater.* **18**, 3613 (2008).
- [6] S. Li, H. Zhang, J. Xu, and D. Yang, *Mater. Lett.* **59**, 420 (2005).
- [7] M. G. Ma and Y. J. Zhu, *J. Nanosci. Nanotech.* **7**, 4552 (2007).
- [8] J. Yu, H. Guo, and B. Cheng, *J. Solid. State. Chem.* **179**, 800 (2006).
- [9] M. X. Zhang, J. C. Huo, Y. S. Yu, C. P. Cui, and Y. L. Lei, *Chin. J. Struct. Chem.* **27**, 1223 (2008).
- [10] M. G. Ma and Y. J. Zhu, *Mater. Lett.* **62**, 2512 (2008).
- [11] I. Sondi and E. Matijević, *Chem. Mater.* **15**, 1322 (2003).
- [12] M. Cao, X. Wu, X. He, and C. Hu, *Langmuir* **21**, 6093 (2005).
- [13] J. J. Shi, J. J. Li, Y. F. Zhu, F. Wei, and X. R. Zhang, *Anal. Chim. Acta.* **466**, 69 (2002).
- [14] K. Omata, N. Nukui, T. Hottai, Y. Showa, and M. Yamada, *Catal. Commun.* **5**, 755 (2004).
- [15] L. Wang and Y. F. Zhu, *J. Phys. Chem. B* **109**, 5118 (2005).
- [16] M. Erdemoglu and M. Canbazoglu, *Hydrometall.* **49**, 135 (1998).
- [17] T. J. Bastow, *Chem. Phys. Lett.* **354**, 156 (2002).
- [18] J. Du, Z. Liu, Z. Li, B. Han, Y. Huang, and J. Zhang, *Micropor. Mesopor. Mater.* **83**, 145 (2005).
- [19] W. S. Wang, L. Zhen, C. Y. Xu, L. Yang, and W. Z. Shao, *Cryst. Growth Des.* **8**, 1734 (2008).
- [20] X. Wang and Y. Li, *Angew. Chem. Int. Ed.* **41**, 4790 (2002).
- [21] S. C. Shen, Q. Chen, P. S. Chow, G. H. Tan, X. T. Zeng, Z. Wang, and R. B. H. Tan, *J. Phys. Chem. C* **111**, 700 (2007).
- [22] W. C. Zhu, Q. Zhang, L. Xiang, F. Wei, X. Sun, X. Piao, and S. Zhu, *Cryst. Growth Des.* **8**, 2938 (2008).
- [23] M. Yoshimura and K. Byrappa, *J. Mater. Sci.* **43**, 2085 (2008).
- [24] Y. Feng, W. Lu, L. Zhang, X. Bao, B. Yue, Y. Lv, X. Shang, *Cryst. Growth Des.* **8**, 1426 (2008).
- [25] L. P. Zhu, G. H. Liao, Y. Yang, H. M. Xiao, J. F. Wang, and S. Y. Fu, *Nanoscale Res. Lett.* **4**, 550 (2009).
- [26] Y. Li, J. Liu, X. Huang, and G. Li, *Cryst. Growth Des.* **7**, 1350 (2007).
- [27] Y. Li, J. Liu, and X. Huang, *Nanoscale Res. Lett.* **3**, 365 (2008).
- [28] C. Chen, X. Sun, X. Jiang, D. Niu, A. Yu, Z. Liu, and J. G. Li, *Nanoscale Res. Lett.* **4**, 971 (2009).
- [29] Y. Li, M. H. Cao, and L. Y. Feng, *Langmuir* **25**, 1705 (2009).
- [30] X. Liu, X. Peng, W. Xie, and Q. Wei, *Chin. J. Mater. Res.* **19**, 287 (2005).
- [31] R. Li, X. Tao, and X. Li, *J. Mater. Chem.* **19**, 983 (2009).